JOURNAL OF Materials CHEMISTRY

Synthesis of aluminium and gallium fluoroalkoxide compounds and the low pressure metal-organic chemical vapor deposition of gallium oxide films

Liliana Mîinea,[a,b] Seigi Suh,[a,b] Simon G. Bott,[a] Jia-Rui Liu,[c] Wei-Kan Chu[c] and David M. Hoffman*[a,b]

[a]*Department of Chemistry,* [b]*Materials Research Science and Engineering Center,* [c]*Texas Center for Superconductivity, University of Houston, Houston, Texas, USA, 77204. E-mail: hoffman@uh.edu*

Received 2nd November 1998, Accepted 15th January 1999

Aluminium and gallium fluoroalkoxide complexes of formula $M(OR_f)_3(HNMe_2)$ [M = Al or Ga; R_f = $CH(CF_3)_2$, $CMe_2(CF_3)$ or $CMe(CF_3)_2$] were prepared by reacting the corresponding metal dimethylamide complexes with fluorinated alcohols. The dimethylamine adducts reacted with 4-dimethylaminopyridine to give $M(OR_f)_3$(4-Me_2Npy) [M = Al or Ga; R_f = $CH(CF_3)_2$, $CMe_2(CF_3)$ or $CMe(CF_3)_2$]. Crystal structure analyses of $Ga[OCH(CF_3)_2]_3$(4-Me_2Npy), $Ga[OCMe_2(CF_3)]_3$(4-Me_2Npy) and $Al[OCMe(CF_3)_2]_3$(4-Me_2Npy) showed they have distorted tetrahedral geometries. Gallium oxide films were prepared from $Ga[OCH(CF_3)_2]_3(HNMe_2)$ and air by low-pressure chemical vapor deposition at substrate temperatures of 250–450 °C. Films deposited at 450 °C had a composition of $Ga_2O_{3.1}$ by backscattering analysis, an optical band gap of 4.9 eV, and were >90% transmittant in the 300–820 nm region.

Gallium oxide films have recently attracted interest because of their application as high temperature gas sensors.[1,2] Although chemical vapor deposition (CVD) is the most practical method to prepare thin films for large-scale applications, there appears to be only one report in the literature in which this method was used to prepare gallium oxide films.[3] In the report, $Ga[CF_3C(O)C(H)C(O)CF_3]_3$ and oxygen were used in a low pressure CVD process to prepare stoichiometric Ga_2O_3 films. Herein we describe the synthesis of new gallium fluoroalkoxide complexes, the use of one of the gallium derivatives to prepare gallium oxide films in a low-pressure CVD process and, in the interest of synthetic completeness, the synthesis of analogous aluminium fluoroalkoxide complexes.

Experimental

Synthesis: general considerations

All manipulations were carried out in a glove box or by using Schlenk techniques. The solvents were purified by using standard methods and stored in the glove box over molecular sieves. The alcohols were obtained commercially. They were degassed with an argon stream and then stored over molecular sieves. Commercial samples of $AlCl_3$ and $GaCl_3$ were purified by sublimation. The compounds $[M(NMe_2)_3]_2$ (M = Al, Ga) were prepared by the literature methods.[4,5] Elemental analyses were performed by Oneida Research Services, Whitesboro, NY.

$Al[OCH(CF_3)_2]_3(HNMe_2)$ 1. An ether solution (15 mL) of $(CF_3)_2CHOH$ (1.7 g, 10 mmol) was added slowly to a solution of $[Al(NMe_2)_3]_2$ (0.50 g, 1.7 mmol) in ether (15 mL) at −34 °C. The reaction mixture was warmed to room temperature and then refluxed for 12 h. The volatile components were removed *in vacuo*, and the residue, a viscous, pale yellow liquid, was distilled under reduced pressure giving $Al[OCH(CF_3)_2]_3(HNMe_2)$ (bp 45–51 °C/0.01 mm Hg) as a colorless liquid (yield 1.4 g, 72%). ^{1}H NMR (C_6D_6): δ 4.4 (septet, 3, $^3J_{HF}$ 6.0 Hz, OC*H*$(CF_3)_2$), 1.5 (s, 6, NMe_2). The N*H* resonance was not located in the spectrum. $^{13}C\{^1H\}$ NMR (C_6D_6): δ 124 (q, 6, $^1J_{CF}$ 280 Hz, OCH(CF_3)$_2$), 72 (septet, 3, $^2J_{CF}$ 33 Hz, O*C*H$(CF_3)_2$), 37 (s, 2, HN(CH_3)$_2$). IR (Nujol, KBr, cm^{-1}): 3300 m [ν(N−H)], 1628 w, 1300 m, 1265 w, 1192 m, 1130 w, 1100 s, 1051 m, 1016 m, 893 s, 856 s, 819 m, 773 m, 686 vs, 570 w, 468 s (Found: C, 22.58; H, 1.51; N, 2.75. Calc. for $C_{11}H_{10}F_{18}NO_3Al$: C, 23.05; H, 1.76; N, 2.44%).

$Ga[OCH(CF_3)_2]_3(HNMe_2)$ 2. A solution of $(CF_3)_2CHOH$ (1.45 g, 8.62 mmol) in ether (5 mL) was added dropwise to a cold (−78 °C) solution of $[Ga(NMe_2)_3]_2$ (0.50 g, 1.44 mmol) in ether (10 mL). After the addition was completed, the reaction mixture was warmed slowly to room temperature and then left to stir overnight. The volatile components were removed *in vacuo* to give the product as a colorless liquid that became a white solid on standing overnight in the dry box (yield 1.56 g, 95%). ^{1}H NMR (C_6D_6): δ 4.70 (septet, 3, $^3J_{HF}$ 5.4 Hz, OC*H*$(CF_3)_2$), 2.78 (br s, 1, *H*NMe_2), 1.63 (s, 6, HN*Me*$_2$). $^{13}C\{^1H\}$ NMR (C_6D_6): 123.1 (q, 6, $^1J_{CF}$ 284 Hz, OCH(CF_3)$_2$), 71.9 (septet, 3, $^2J_{CF}$ 33 Hz, O*C*H$(CF_3)_2$), 37.3 (s, 2, HN*Me*$_2$). IR (Nujol, CsI, cm^{-1}): 3298 m [ν(N−H)], 1292 s, 1190 (br) s, 1097 s, 1028 m, 895 s, 868 s, 760 m, 685 s, 523 m (Found: C, 21.48; H, 1.66; N, 2.43. Calc. for $C_{11}H_{10}F_{18}NO_3Ga$: C, 21.44; H, 1.64; N, 2.27%).

$Al[OCMe_2(CF_3)]_3(HNMe_2)$ 3. An ether solution (15 mL) of $(CF_3)Me_2COH$ (2.4 g, 18 mmol) was added dropwise to a cold (0 °C) solution of $[Al(NMe_2)_3]_2$ (0.84 g, 2.9 mmol) in ether (20 mL). The reaction mixture was stirred for 15 h while the temperature was allowed to increase slowly to room temperature. The volatile components were removed *in vacuo*, and the residue, a viscous, pale yellow liquid, was distilled under reduced pressure to give $Al[OCMe_2(CF_3)]_3(HNMe_2)$ (bp 82 °C/0.01 mm Hg) as a colorless liquid (yield 1.95 g, 75%). ^{1}H NMR (C_6D_6): δ 1.7 (d, 6, J_{HH} 6.3 Hz, N*Me*$_2$), 1.4 (s, 18, OC(CH_3)$_2$(CF_3)). The N*H* resonance could not be identified in the spectrum. $^{13}C\{^1H\}$ NMR (C_6D_6): δ 128 (q, 3, $^1J_{CF}$ 285 Hz, OC(CH_3)$_2$(*C*F_3)), 72 (q, 3, $^2J_{CF}$ 28 Hz, O*C*(CH_3)$_2$(CF_3)), 37 (s, 2, HN(CH_3)$_2$), 26 (s, 6, OC(*C*H_3)$_2$(CF_3)). IR (Nujol, KBr, cm^{-1}): 3302 s [ν(N−H)],

1327 m, 1230 w, 1157 s, 1059 m, 995 m, 906 s, 777 s, 644 m, 606 s, 555 w, 478 sh.

$Ga[OCMe_2(CF_3)]_3(HNMe_2)$ 4. An ether solution (10 mL) of $(CF_3)Me_2COH$ (1.2 g, 9.7 mmol) was added dropwise to a cold (0 °C) solution of $[Ga(NMe_2)_3]_2$ (0.60 g, 1.5 mmol) in ether (40 mL). The reaction mixture was stirred for 15 h while the temperature was allowed to increase slowly to room temperature. The volatile components were removed *in vacuo*, and the residue, a viscous, pale yellow liquid, was distilled at low pressure giving $Ga[OCMe_2(CF_3)]_3(HNMe_2)$ (bp 77–80 °C/0.01 mm Hg) as a colorless liquid (yield 0.92 g, 62%). ^1H NMR (C_6D_6): δ 1.69 (d, 6, J_{HH} 6.0 Hz, NMe_2), 1.42 (s, 18, OC(CH_3)$_2$(CF_3)). The NH resonance could not be identified in the spectrum. $^{13}C\{^1H\}$ NMR (C_6D_6): δ 128 (q, 3, $^1J_{CF}$ 284 Hz, OC(CH_3)$_2$(CF_3)), 74 (q, 3, $^2J_{CF}$ 28 Hz, OC(CH_3)$_2$(CF_3)), 37 (s, 2, HN(CH_3)$_2$), 26 (s, 6, OC(CH_3)$_2$(CF_3)). IR (Nujol, KBr, cm^{-1}): 3310 m [ν(N–H)], 1420 w, 1352 m, 1290 vw, 1204 s, 1153 vs, 1130 vs, 1072 w, 1043 w, 1018 m, 891 s, 841 w, 800 w, 763 m, 613 s, 462 vs.

$Al[OCMe(CF_3)_2]_3(HNMe_2)$ 5. An ether solution (15 mL) of $(CF_3)_2MeCOH$ (3.3 g, 18 mmol) was added slowly to a solution of $[Al(NMe_2)_3]_2$ (0.66 g, 2.2 mmol) in ether (15 mL) at room temperature. After the addition was completed, the reaction mixture was refluxed for 6 h. The volatile components were removed *in vacuo*, and the residue, a viscous pale yellow liquid, was distilled under reduced pressure giving $Al[OCMe(CF_3)_2]_3(HNMe_2)$ (bp 68–72 °C/0.01 mmHg) as a colorless liquid (yield 1.9 g, 64%). ^1H NMR (C_6D_6): δ 1.6 (d, 6, J_{HH} 6.0 Hz, NMe_2), 1.4 (s, 9, OC(CH_3)(CF_3)$_2$), 1.2 (br, 1, NH). $^{13}C\{^1H\}$ NMR (C_6D_6): δ 125 (q, 6, $^1J_{CF}$ 285 Hz, OC(CF_3)$_2$(CH_3)), 76 (septet, 3, $^2J_{CF}$ 30 Hz, OC(CF_3)$_2$(CH_3)), 37 (s, 2, HN(CH_3)$_2$), 19 (s, 3, OC(CF_3)$_2$(CH_3)). IR (Nujol, KBr, cm^{-1}): 3296 m [ν(N–H)], 1309 m, 1244 s, 1202 s, 1119 m, 1084 s, 1049 w, 1013 m, 952 w, 891 w, 868 w, 806 m, 702 s, 661 w, 621 m.

$Ga[OCMe(CF_3)_2]_3(HNMe_2)$ 6. A solution of $(CF_3)_2MeCOH$ (2.6 g, 14 mmol) in ether (10 mL) was added slowly to a solution of $[Ga(NMe_2)_3]_2$ (0.92 g, 2.2 mmol) in ether (25 mL) at room temperature. The reaction mixture was then refluxed for 16 h. The volatile components were removed *in vacuo*, and the residue, a viscous pale yellow liquid, was distilled under reduced pressure giving $Ga[OCMe(CF_3)_2]_3(HNMe_2)$ (bp 91–97 °C/0.01 mm Hg) as a colorless liquid which turns to a white solid at room temperature (yield 1.3 g, 59%). ^1H NMR (C_6D_6): δ 1.6 (d, 6, J_{HH} 6.0 Hz, NMe_2), 1.5 (s, 9, OC(CH_3)(CF_3)$_2$), 1.3 (br, 1, NH). $^{13}C\{^1H\}$ NMR (C_6D_6): δ 124 (q, 6, $^1J_{CF}$ 286 Hz, OC(CF_3)$_2$(CH_3)), 77 (septet, 3, $^2J_{CF}$ 29 Hz, OC(CF_3)$_2$(CH_3)), 37 (s, 2, HN(CH_3)$_2$), 19 (s, 3, OC(CF_3)$_2$(CH_3)). IR (Nujol, KBr, cm^{-1}): 3308 m [ν(N–H)], 1311 s, 1224 w, 1180 s, 1118 s, 1076 vs, 1018 s, 977 vs, 866 m, 771 s, 623 s.

$Al[OCH(CF_3)_2]_3$(4-Me_2Npy) 7. The compound 4-Me_2Npy (0.040 g, 0.33 mmol) was added to a solution of $Al[OCH(CF_3)_2]_3(HNMe_2)$ (0.20 g, 0.35 mmol) in ether (15 mL) at room temperature. The reaction mixture was stirred for 12 h. The solvent and $HNMe_2$ were removed *in vacuo*, and the residue, a white solid, was washed with hexanes (2 × 15 mL) and then dried under vacuum (yield 0.20 g, 91%). Despite several attempts, crystals suitable for X-ray crystallographic analysis could not be obtained. ^1H NMR (C_6D_6): δ 7.8 (d, 2, J_{HH} 7.5 Hz, H^2, H^6 of C_5H_4N), 5.3 (d, 2, J_{HH} 7.5 Hz, H^3, H^5 of C_5H_4N), 4.8 (septet, 3, $^3J_{HF}$ 6.0 Hz, OCH(CF_3)$_2$), 1.8 (s, 6, NMe_2). IR (Nujol, KBr, cm^{-1}): 1639 vs, 1564 s, 1531 w, 1406 w, 1292 s, 1271 s, 1228 s, 1184 s, 1099 s, 1080 m, 1031 s, 947 w, 891 m, 854 s, 820 s, 773 m, 707 w, 686 vs, 682 m, 522 w (Found: C, 29.43; H, 1.89; N, 4.21. Calc. for $C_{16}H_{13}F_{18}N_2O_3Al$: C, 29.54; H, 2.02; N, 4.30%).

$Ga[OCH(CF_3)_2]_3$(4-Me_2Npy) 8. The compound $Ga[OCH(CF_3)_2]_3(HNMe_2)$ was generated *in situ* following the procedure given above. Ether/hexanes (1 : 1, 10 mL) was added to the dimethylamine adduct, followed by 4-dimethylaminopyridine (0.19 g, 1.58 mmol). A white solid precipitated slowly from the solution. After stirring overnight, the mixture was taken to dryness *in vacuo* to give a pale yellow solid. The solid was crystallized as colorless blocks from an ether solution at −35 °C [yield 0.87 g, 80% based on $Ga(NMe_2)_3$]. A satisfactory carbon analysis was not obtained. ^1H NMR (C_6D_6): δ 7.67 (d, 2, H^2, H^6 of C_5H_4N), 5.27 (d, 2, H^3, H^5 of C_5H_4N), 5.01 (septet, 3, $^3J_{HF}$ 6.1 Hz, OCH(CF_3)$_2$), 1.79 (s, 6, NMe_2). $^{13}C\{^1H\}$ NMR (C_6D_6): 156 (s, 1, C^4 of C_5H_4N), 145 (s, 2, C^2, C^6 of C_5H_4N), 124 (q, 6, $^1J_{CF}$ 283 Hz, OCH(CF_3)$_2$), 107 (s, 2, C^3, C^5 of C_5H_4N), 72.2 (septet, 3, $^2J_{CF}$ 33 Hz, OCH(CF_3)$_2$), 38.1 (s, 2, NMe_2). IR (Nujol, KBr, cm^{-1}): 1636 s, 1562 m, 1287 s, 1227 s, 1188 s, 1098 s, 1030 m, 1016 m, 889 m, 858 m, 819 m, 760 m, 685 m (Found: C, 28.96; H, 1.81; N, 3.98. Calc. for $C_{16}H_{13}F_{18}N_2O_3Ga$: C, 27.73; H, 1.88; N, 4.04%).

$Al[OCMe_2(CF_3)]_3$(4-Me_2Npy) 9. The compound 4-Me_2Npy (0.12 g, 0.98 mmol) was added to a solution of $Al[OCMe_2(CF_3)]_3(HNMe_2)$ (0.47 g, 1.0 mmol) in ether (15 mL) at room temperature. After the reaction mixture was stirred for 12 h, the volatile components were removed *in vacuo*. The residue, a white solid, was dissolved in a minimum amount of CH_2Cl_2 (5 mL) and the flask was placed in the freezer (−34 °C). This produced colorless crystals (yield 0.45 g, 88%). Crystals could also be grown from hexanes/ether and hexanes/CH_2Cl_2 at low temperature. A satisfactory nitrogen analysis was not obtained. ^1H NMR (C_6D_6): δ 8.2 (d, 2, J_{HH} 6.0 Hz, H^2, H^6 of C_5H_4N), 5.5 (d, 2, J_{HH} = 7.5 Hz, H^3, H^5 of C_5H_4N), 1.77 (s, 6, NMe_2), 1.59 (s, 18, OC(CF_3)(CH_3)$_2$). IR (Nujol, KBr, cm^{-1}): 1632 s, 1562 m, 1531 w, 1327 m, 1256 w, 1229 s, 1151 vs, 1128 vs, 1076 m, 1049 w, 1030 m, 995 w, 947 w, 902 m, 825 m, 775 m, 700 m, 644 w, 606 m, 553 w (Found: C, 43.07; H, 5.31; N, 5.88. Calc. for $C_{19}H_{28}F_9N_2O_3Al$: C, 42.98; H, 5.28; N, 5.28%).

$Ga[OCMe_2(CF_3)]_3$(4-Me_2Npy) 10. The compound 4-Me_2Npy (0.16 g, 1.34 mmol) was added to a solution of $Ga[OCMe_2(CF_3)]_3(HNMe_2)$ (0.70 g, 1.4 mmol) in ether (15 mL) at room temperature. The reaction mixture was stirred for 12 h, and the solvent and $HNMe_2$ were then removed *in vacuo*. The residue, a white solid, was dissolved in a minimum amount of CH_2Cl_2 (5 mL) and the flask was placed in the freezer (−34 °C). This produced colorless crystals (yield 0.67 g, 87%). Crystals could also be grown from hexanes/ether and hexanes/CH_2Cl_2 at low temperature. ^1H NMR (C_6D_6): δ 8.1 (d, 2, J_{HH} 7.8 Hz, H^2, H^6 of C_5H_4N), 5.4 (d, 2, J_{HH} 6.9 Hz, H^3, H^5 of C_5H_4N), 1.8 (s, 6, NMe_2), 1.6 (s, 18, OC(CF_3)(CH_3)$_2$). IR (Nujol, KBr, cm^{-1}): 1629 vs, 1553 s, 1327 m, 1205 s, 1150 vs, 1078 s, 1028 s, 949 w, 889 m, 761 w, 648 w, 613 w (Found: C, 40.02; H, 4.94; N, 4.93. Calc. for $C_{19}H_{28}F_9N_2O_3Ga$: C, 39.78; H, 4.88; N, 4.88%).

$Al[OCMe(CF_3)_2]_3$(4-Me_2Npy) 11. The compound 4-Me_2Npy (0.057 g, 0.47 mmol) was added to a solution of $Al[OCMe(CF_3)_2]_3(HNMe_2)$ (0.30 g, 0.49 mmol) in ether (15 mL) at room temperature. The reaction mixture was stirred for 12 h. The solvent and $HNMe_2$ were removed *in vacuo*, and the residue, a white solid, was washed with hexanes (2 × 15 mL) and dried under vacuum (yield 0.28 g, 89%). ^1H NMR (C_6D_6): δ 8.0 (d, J_{HH} 6.0 Hz, 2, H^2, H^6 of C_5H_4N), 5.4 (d, J_{HH} 6.0 Hz, 2, H^3, H^5 of C_5H_4N), 1.7 (s, 6, NMe_2), 1.6 (s, 9, OC(CH_3)(CF_3)$_2$). IR (Nujol, KBr, cm^{-1}): 1636 s, 1560 m,

1537 w, 1402 w, 1386 m, 1321 w, 1307 s, 1234 s, 1198 vs, 1138 w, 1117 m, 1082 s, 1034 m, 1005 m, 949 w, 868 m, 821 m, 798 w, 775 w, 740 w, 702 s, 621 w (Found: C, 32.86; H, 2.73; N, 4.43. Calc. for $C_{19}H_{19}F_{18}N_2O_3Al$: C, 32.93; H, 2.74; N, 4.04%).

$Ga[OCMe(CF_3)_2]_3(4\text{-}Me_2Npy)$ 12. The compound 4-Me_2Npy (0.15 g, 1.2 mmol) was added to a solution of $Ga[OCMe(CF_3)_2]_3(HNMe_2)$ (0.86 g, 1.3 mmol) in ether (20 mL) at room temperature. The reaction mixture was stirred for 12 h. The solvent and $HNMe_2$ were removed *in vacuo*, and the residue, a white solid, was washed with hexanes (2 × 15 mL) and then dried under vacuum (yield 0.76 g, 83%). Colorless crystals were grown from a mixture of hexanes/CH_2Cl_2 (1:3). ^{1}H NMR (C_6D_6): δ 8.0 (d, 2, J_{HH} 7.5 Hz, H^2, H^6 of C_5H_4N), 5.3 (d, 2, J_{HH} 7.5 Hz, H^3, H^5 of C_5H_4N), 1.8 (s, 6, NMe_2), 1.7 (s, 9, OC(CH_3)(CF_3)$_2$). IR (Nujol, KBr, cm^{-1}): 1632 vs, 1556 s, 1535 w, 1402 m, 1303 s, 1225 m, 1196 s, 1135 w, 1116 w, 1080 m, 1031 m, 977 s, 949 w, 868 m, 821 m, 770 m, 702 s, 623 w (Found: C, 30.93; H, 2.63; N, 3.81. Calc. for $C_{19}H_{19}F_{18}N_2O_3Ga$: C, 31.02; H, 2.61; N, 3.81%).

X-Ray crystallographic studies

Compound 11. The sample for analysis was grown at low temperature (−35 °C) from CH_2Cl_2. The crystals were manipulated under mineral oil during the mounting procedure. The selected crystal, a colorless parallelepiped, was mounted on a glass fiber attached to a goniometer. The goniometer was then moved to the diffractometer cold stream. Measurements were made with a Siemens SMART platform diffractometer equipped with a 1K CCD area detector. A hemisphere of data (1271 frames at 5 cm detector distance) was collected using a narrow-frame method with scan widths of 0.30% in omega and an exposure time of 15 s per frame. The first 50 frames were re-measured at the end of data collection to monitor instrument and crystal stability, and the maximum correction on I was <1%. During data reduction the intensities were corrected for Lorentz factor, polarization, air absorption and absorption due to variation in the path length through the detector faceplate. A psi scan absorption correction was applied based on the entire data set. Redundant reflections were averaged. Final cell constants were refined using 4918 reflections having $I > 10\sigma(I)$. The Laue symmetry was determined to be $\bar{1}$, and the space group was shown to be either $P1$ or $P\bar{1}$. Since the unitary structure factors displayed centric statistics, space group $P\bar{1}$ was assumed from the outset. The structure was solved by direct methods. The hydrogens were included in idealized positions.

Compounds 8 and 10. Colorless blocks of **8** and **10** were grown at low temperature (−35 °C) from ether and CH_2Cl_2, respectively. The crystals were mounted under argon in capillaries. After mounting the crystal of **10**, it was white rather than colorless, suggesting there was surface decomposition. Data were collected on an Enraf-Nonius CAD-4 diffractometer (Mo-Kα, $\lambda = 0.71073$ Å) using the $\theta/2\theta$ (**8**) and ω–2θ (**10**) scan techniques. Three standard reflections were monitored after every 3600 s of exposure time and these showed no significant decay. During data reduction, Lorentz and polarization corrections were applied as well as absorption corrections (**8**, DIFABS; **10**, psi scans). In both cases, the crystals were weak scatterers.

The structures were solved by interpretation of Patterson maps, which revealed the positions of the Ga atoms. Remaining non-hydrogen atoms were located in subsequent difference Fourier syntheses. The usual sequence of isotropic and anisotropic refinement was followed. In both cases only the Ga and F atoms were treated with anisotropic thermal parameters due to a lack of data. The hydrogens were included in idealized positions [$U(H) = 1.3\ B_{eq}(C)$]. For **8** no unusually high correlation was noted between any of the variables in the last cycle of full matrix least squares refinement. The final difference density map showed a maximum peak of about 0.42 e A^{-3} located near O11. For **10**, one $CMe_2(CF_3)$ group was found to be disordered over two sites (site occupancies of 2:1). The final difference density map showed a maximum peak of about 0.54 e A^{-3} located near O3. All computations were performed using the MolEN structure solution package of programs.[6]

CCDC reference number 1145/140.

Thin film depositions

Depositions were carried out in a cold-walled low-pressure glass reactor (**I**). The base pressure for the system was

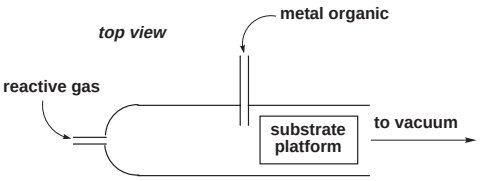

I

1.7–2.0 × 10^{-2} Torr. Air was admitted to the reactor *via* a Teflon bleed valve. When oxygen (extra dry grade) was used as the reactant gas, it was diluted with helium (ultra high purity) (40 sccm O_2 in 160 sccm He). The precursor $Ga[OCH(CF_3)_2]_3(HNMe_2)$ was used as produced from its synthesis (purity by NMR >98%). The precursor bubbler and feed line were maintained at 100–115 °C by using heating tape. The deposition pressure was 0.48–0.50 Torr. After the bubbler was shut off for a given run, the films were left at low pressure under a flow of air for 3 min while maintaining the deposition temperature. The films were then cooled rapidly under the flow of air.

Film characterization

Backscattering spectrometry was used to determine film elemental composition (Ga, C, N, F and O) and thickness. Data were acquired at the Texas Center for Superconductivity on a NEC Pellepron C-type tandem accelerator using a 3.48 MeV $^4He^{2+}$ beam. The data were modeled using the program RUMP.[7] Infrared spectra were collected on a Mattson Galaxy 5000 FT-IR in the 400–4000 cm^{-1} range, and transmittance spectra were collected on a Hewlett-Packard 8452A diode array spectrophotometer.

Results and discussion

Syntheses and spectroscopic characterization

A summary of our synthetic results is presented in Scheme 1.

The compounds $[M(NMe_2)_3]_2$ (M = Al or Ga) react with fluorinated alcohols (R_fOH) to give the dimethylamine adducts $M(OR_f)_3(HNMe_2)$ [$R_f = CH(CF_3)_2$, M = Al (**1**) or Ga (**2**); $R_f = CMe_2(CF_3)$, M = Al (**3**) or Ga (**4**); R_f = $CMe(CF_3)_2$, M = Al (**5**) or Ga (**6**)] in moderate to high yield. In general, purification of the compounds is difficult and only after repeated preparations were compounds obtained that gave clean NMR spectra. The compounds are moderately air sensitive, volatile colorless liquids that distill at <100 °C under reduced pressure. In pure form **2** and **6** solidify at room temperature. The fact that the amine ligands were not lost during low-pressure distillation indicates they are held tightly. Also, the $HNMe_2$ ligand in **4** was not removed under the more vigorous conditions of refluxing a toluene solution under argon for 63 h. If the reactions to form **1** and **5** are carried

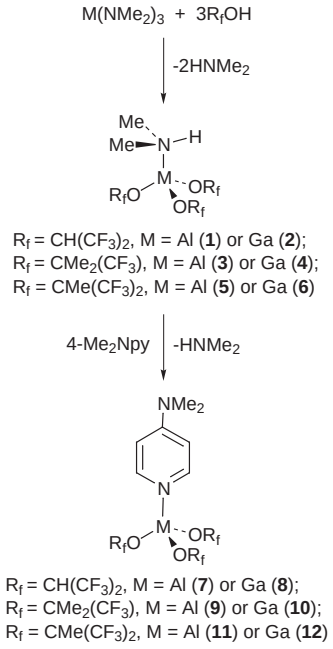

Scheme 1

out at or below room temperature, mixtures of compounds, which from NMR spectra appear to be composed of the neutral amine adducts and the salts $[Me_2NH_2]\{Al[OR_f]_4\}$, are formed.

In ^{1}H NMR spectra of the dimethylamine adducts, the HN*Me*$_2$ protons are doublets due to coupling to the amine proton. Spectra for compounds **1** and **2**, in which the methyl protons appear as singlets, are exceptions. For compounds **2**, **5** and **6**, the *H*NMe$_2$ protons give rise to broad resonances while for **1**, **3** and **4** the resonances are too broad to be definitively identified in the spectra. All the compounds give rise to an IR band at $\approx$3300 cm^{-1} that can be assigned to an N–H stretch. In ^{13}C{^{1}H} NMR spectra ^{13}C–^{19}F coupling is observed both for *C*F$_3$ groups ($^1J_{CF} \approx 285$ Hz) and tertiary carbons ($^2J_{CF} \approx 30$ Hz).

Purification of the dimethylamine adducts was difficult because it was necessary to handle small quantities of the liquids. Solid derivatives were synthesized (Scheme 1) to make purification easier and to have samples for X-ray analysis. The solid samples were prepared by reacting the adducts with *p*-dimethylaminopyridine to give displacement of dimethylamine and formation of M(OR$_f$)$_3$(4-Me$_2$Npy) [R$_f$=CH(CF$_3$)$_2$, M=Al (**7**) or Ga (**8**); R$_f$=CMe$_2$(CF$_3$), M=Al (**9**) or Ga (**10**); R$_f$=CMe(CF$_3$)$_2$, M=Al (**11**) or Ga (**12**)]. Compounds **7**–**12** can be isolated as colorless crystals by low temperature crystallization. Proton NMR spectra for all the compounds are consistent with the solid state structures of **8**, **10** and **11** (see below).

X-Ray crystallographic studies

X-Ray crystallographic studies on **8**, **10** and **11** were carried out. Plots are shown in Fig. 1 (**8**), 2 (**10**) and 3 (**11**), crystal data are given in Table 1, and selected bond distances and angles are presented in Table 2. The crystals of **8** and **10** were poor scatterers, which was detrimental to the quality of the results.

The molecules are distorted tetrahedra with O–M–O and O–M–N angles ranging from 102.4 to 117.0°. The Ga–O bond distances (average 1.80 Å) are statistically equivalent by the 3σ criterion and they are on average about 0.08 Å longer than the corresponding Al–O distances. The Ga–O distances are somewhat shorter than the terminal Ga–O distances in the four-coordinate compounds (Bu^t)$_2$Ga(OBu^t)(O=AsPh$_3$) [1.860(6) Å][8] and Me$_2$Ga[O(C$_5$H$_3$N)CH$_2$NMe$_2$] [1.892(3) Å][9] and about the same as those in three-coordinate (Bu^t)$_2$GaOR where R=2,6-Bu$^t_2$-4-MeC$_6$H$_2$ [1.821(3) Å][10] and CPh$_3$ [1.831(4) Å].[11] The Ga–N distances, 1.924(7) and 1.97(1) Å, are significantly shorter than in Me$_2$Ga[O(C$_5$H$_3$N)CH$_2$NMe$_2$] [2.127(4) Å] and dative Ga–N

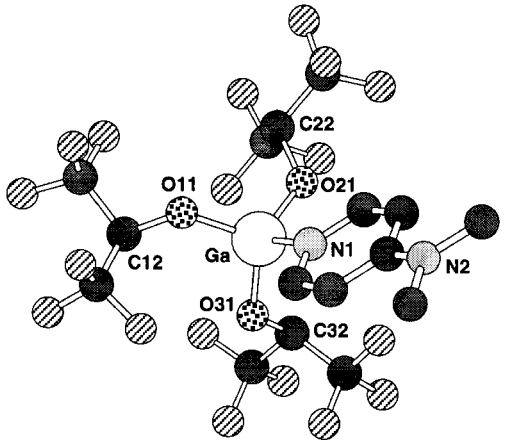

Fig. 1 Ball-and-stick plot of Ga[OCH(CF$_3$)$_2$]$_3$(4-Me$_2$Npy) **8** showing the atom numbering scheme.

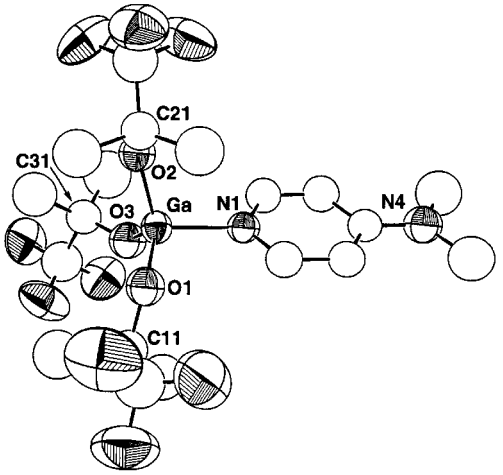

Fig. 2 Plot of Ga[OCMe$_2$(CF$_3$)]$_3$(4-Me$_2$Npy) **10** showing the atom numbering scheme (40% probability ellipsoids except for carbon atoms, which are shown as spheres of arbitrary radius).

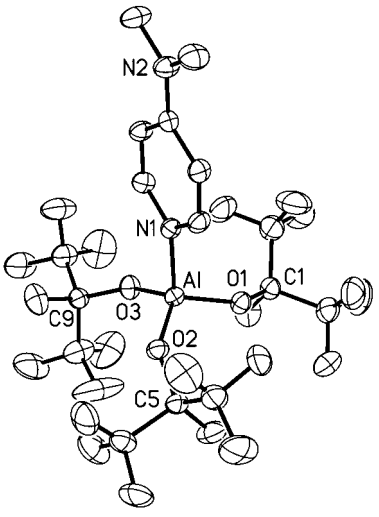

Fig. 3 Plot of Al[OCMe(CF$_3$)$_2$]$_3$(4-Me$_2$Npy) **11** showing the atom numbering scheme (40% probability ellipsoids).

Table 1 Crystal data for $Ga[OCH(CF_3)_2]_3(4\text{-}Me_2Npy)$ **8**, $Ga[OCMe_2(CF_3)]_3(4\text{-}Me_2Npy)$ **10** and $Al[OCMe(CF_3)_2]_3(4\text{-}Me_2Npy)$ **11**

Compound	**8**	**10**	**11**
Formula	$C_{16}H_{13}F_{18}GaN_2O_3$	$C_{19}H_{28}F_9GaN_2O_3$	$C_{19}H_{19}F_{18}AlN_2O_3$
M	692.98	573.15	692.34
Crystal dimensions (mm)	$0.21\times0.23\times0.24$	$0.11\times0.13\times0.14$	$0.40\times0.40\times0.32$
Space group	$P\bar{1}$ (triclinic)	$P\bar{1}$ (triclinic)	$P\bar{1}$ (triclinic)
a/Å	9.8702(8)	9.8968(7)	9.9519(7)
b/Å	0.1494(8)	1.539(2)	11.9185(8)
c/Å	13.858(1)	12.692(2)	12.8978(9)
α/deg	85.426(6)	66.90(1)	65.4720(10)
β/deg	74.849(6)	76.819(9)	77.2940(10)
γ/deg	67.852(6)	86.733(9)	83.3810(10)
T/°C	23	23	−50
Z	2	2	2
V/Å^3	1240.8(2)	1297.2(3)	1357.20(16)
D_{calcd}/g cm^{-3}	1.855	1.467	1.694
μ/cm^{-1}	12.56	11.39	2.24
Reflections measured (unique)	3042 (3042)	3169(3169)	6045(3796)
Reflections observed $[I>n\sigma(I)]$	1814 ($n=3$)	1431 ($n=3$)	3558 ($n=4$)
R, R_w	0.045, 0.046[a]	0.0620, 0.0687[a]	0.0360, 0.0940[b]

[a] $R=\Sigma||F_o|-|F_c||/\Sigma|F_o|$, $R_w=[\Sigma w(|F_o|-|F_c|)^2/\Sigma w|F_o|^2]^{1/2}$, $w=[0.04F^2+(\sigma(F))^2]^{-1}$. [b] $R=\Sigma||F_o|-|F_c||/\Sigma|F_o|$; $R_w=[\Sigma w(F_o^2-F_c^2)^2/\Sigma w(F_o^2)^2]^{1/2}$, $w=[\sigma^2(F_o^2)+(0.0370P)^2+(1.2300P)]^{-1}$ where $P=(F_o^2+2F_c^2)/3$.

Table 2 Selected bond distances (Å) and angles (°) for $Ga[OCH(CF_3)_2]_3(4\text{-}Me_2Npy)$ **8**, $Ga[OCMe_2(CF_3)]_3(4\text{-}Me_2Npy)$ **10** and $Al[OCMe(CF_3)_2]_3(4\text{-}Me_2Npy)$ **11**

	8	**10**	**11**
M–O(n)	1.804(5) ($n=11$)	1.802(8) ($n=1$)	1.7208(15) ($n=1$)
M–O(n)	1.801(5) ($n=21$)	1.80(1) ($n=2$)	1.7205(15) ($n=2$)
M–O(n)	1.811(5) ($n=31$)	1.778(9) ($n=3$)	1.7181(15) ($n=3$)
M–N(1)	1.924(7)	1.97(1)	1.9178(18)
O(n)–M–O(m)	115.0(2) ($n=11$, $m=12$)	110.3(4) ($n=1$, $m=2$)	111.24(8) ($n=1$, $m=2$)
O(n)–M–O(m)	110.5(2) ($n=11$, $m=31$)	117.0(4) ($n=1$, $m=3$)	111.87(8) ($n=1$, $m=3$)
O(n)–M–O(m)	112.0(2) ($n=21$, $m=31$)	114.2(5) ($n=2$, $m=3$)	116.12(8) ($n=2$, $m=3$)
O(n)–M–N(1)	104.7(2) ($n=11$)	104.5(4) ($n=1$)	107.27(8) ($n=1$)
O(n)–M–N(1)	102.8(3) ($n=21$)	107.1(4) ($n=2$)	103.66(8) ($n=2$)
O(n)–M–N(1)	111.4(2) ($n=31$)	102.4(4) ($n=3$)	105.80(8) ($n=3$)
M–O(n)–C(m)	124.2(4) ($n=11$, $m=12$)	130.7(7) ($n=1$, $m=11$)	139.98(14) ($n=1$, $m=1$)
M–O(n)–C(m)	126.9(5) ($n=21$, $m=22$)	126.7(9) ($n=2$, $m=21$)	140.67(14) ($n=2$, $m=5$)
M–O(n)–C(m)	122.7(5) ($n=31$, $m=32$)	133.4(9) ($n=3$, $m=31$)	141.87(14) ($n=3$, $m=9$)

bonds in 5-coordinate Ga compounds.[9] The shorter Ga–N distances are a consequence of the 4-NMe_2 donor group on the pyridine, which enhances the electron donating ability of the pyridine nitrogen lone pair.

The Al–O distances in **11** are within the wide range of Al–O distances [1.687(8)–1.833(8) Å] reported in the 4-coordinate Al alkoxide complexes $Al(OC_6H_3Pr^i_2\text{-}2,6)_3py$,[12] $AlMe(OMes)_2(3,5\text{-}Me_2py)$,[12] $Al(OBu^t)_3(HNMe_2)$,[13] $Al(OR)_3$-$[O=C(C_5H_9)\text{-}4\text{-}Bu^t]$,[14] $AlH_2(OR)(NMe_3)$,[14] $AlH(OR)_2(OEt_2)$,[14] $AlH(OR)_2(H_2NBu^t)$,[14] $AlMe_2(OR)(py)$,[12] $AlMe_2(OR)$-(PMe_3),[15] $AlMe_2(OR)(2,6\text{-}Me_2py)$,[16] $AlMe_2(OC_6F_5)$-$[N(C_2H_4)_3CH]$,[16] $AlMe_2(OR)(O=CPh_2)$,[17] $AlEt_2(OR)$-(H_2NBu^t),[16] $AlEt_2(OR)(py\text{-}N\text{-}O)$,[16] $AlEt_2(OR)[O=C(OMe)C_6$-$H_4\text{-}p\text{-}Me]$,[18] $AlMe(OR)_2(py\text{-}N\text{-}O)$,[16] $AlMe(OR)_2[O=C(OMe)$-$Ph]$,[17] $AlMe(OR)_2[O=C(H)Bu^t]$ ($R=C_6H_2\text{-}2,6\text{-}Bu^t_2\text{-}4\text{-}Me$),[17] and $[Al_4(\mu_4\text{-}O)(\mu\text{-}OCH_2CF_3)_5(OCH_2CF_3)_6]^-$,[19] but they are slightly longer than those in three-coordinate $AlMe(OC_6H_2$-$2,6\text{-}Bu^t_2\text{-}4\text{-}Me)_2$ [average 1.686(2) Å][18] and $Al(OC_6H_2\text{-}2,6$-$Bu^t_2\text{-}4\text{-}Me)_3$ [average 1.648(7) Å],[14] where π bonding is more important. Perhaps a better comparison is to $Al_2(\mu\text{-}NMe_2)(\mu$-$OBu^t)(OBu^t)_4$ and $[Al(OBu^t)_2(\mu\text{-}OBu^t)]_2$ in which the terminal Al–O distances average 1.684(4) and 1.6879(30) Å, respectively.[13,20] The partially fluorinated *tert*-butoxide in **11** may give slightly longer Al–O distances compared to $Al_2(\mu$-$NMe_2)(\mu\text{-}OBu^t)(OBu^t)_4$ and $[Al(OBu^t)_2(\mu\text{-}OBu^t)]_2$ because of the electron withdrawing nature of the CF_3 group.

The M–O–C angles in **11** are significantly larger than those in the two gallium derivatives. This is a consequence of greater steric crowding in the aluminium compound, which in turn is due to the shorter M–O distances for Al compared to Ga.

CVD studies. Depositions using $Ga[OCH(CF_3)_2]_3(HNMe_2)$

Low pressure CVD using **2** and air gave films at substrate temperatures of 250 to 450 °C. The films had a shiny appearance and they adhered well to the substrates as judged by the Scotch tape test. An X-ray diffraction pattern for a film deposited at 450 °C on glass indicated the film was amorphous. Attempted depositions using **2** alone or in combination with dry O_2 diluted with argon did not give films in the same temperature range. This indicates water vapor is the critical reactant in the **2**/air precursor system.

Analyses of backscattering spectra for the films (*e.g.*, Fig. 4) gives O/Ga ratios of 1.6–1.8 with the ratio decreasing as the temperature of deposition is increased (Table 3). Carbon, nitrogen and fluorine peaks are not observed in the spectra, indicating low levels of these elements in the films (<3 atom%). Previously we had shown that depositions of tin oxide thin

Table 3 Compositions and growth rates of films deposited from $Ga[OCH(CF_3)_2]_3(HNEt_2)$ and air

Deposition temperatures/°C	Composition[a]	Growth rate/Å min^{-1}
250	$Ga_2O_{3.5}$	–
300	$Ga_2O_{3.6}$	–
350	$Ga_2O_{3.4}$	2700
400	$Ga_2O_{3.2}$	3300
450	$Ga_2O_{3.1}$	3800

[a]From backscattering spectra. The error is estimated to be ±0.1.

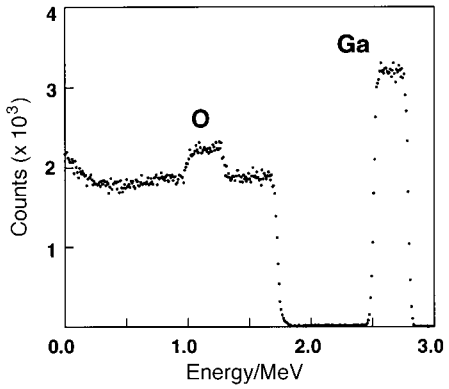

Fig. 4 Backscattering spectrum for a gallium oxide film deposited at 400 °C on silicon. Beam: 3.48 MeV He^{2+}.

films from $Sn[OCH(CF_3)_2]_4(HNMe_2)_2$ and air also gave films having very little fluorine incorporation (F/Sn = 0.005–0.026 by nuclear reaction analysis).[21] The deposition of Ga_2O_3 films from **2** and air probably proceeds *via* hydrolysis of the Ga–OR_f bonds to form =Ga–OH containing intermediates. Incomplete decomposition of these intermediates may account for the excess oxygen in the films. Transmission IR spectra show a very broad band around 3400 cm^{-1} that may be due to the O–H stretch.

Film thicknesses obtained from the backscattering spectra indicate film growth rates increased slightly between 350 and 450 °C (Table 3). Growth rates at 250 and 300 °C could not be reliably calculated because most of the film growth occurred downstream of the substrate, which could not be placed at the site of maximal growth because of the reactor design.

Transmission spectra for 6000–7000 Å thick films grown on quartz slides are shown in Fig. 5. The absorption edges of the films deposited at lower temperatures are shifted to higher energy compared to the film deposited at 400 °C. All the films were >90% transmittant in the mid-ultraviolet and visible regions. Optical bandgaps were calculated from the absorbance data by plotting α^2 *vs.* E and extrapolating the linear portion of the curve to $\alpha^2 = 0$, where α is the absorption coefficient and E is the photon energy. The procedure gives optical band gaps of 5.65, 5.33 and 4.90 eV for the films deposited at 250, 350 and 450 °C, respectively. The reported value for bulk material is 4.8 eV.[22]

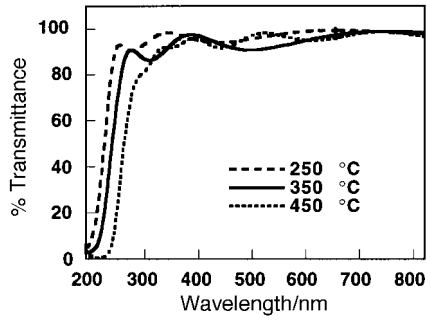

Fig. 5 Transmission spectra of gallium oxide films deposited at 250, 350 and 450 °C on quartz.

Conclusion

Homoleptic aluminium and gallium dimethylamide complexes react with fluorinated alcohols to give $M(OR_f)_3(HNMe_2)$ [M = Al or Ga; $R_f = CH(CF_3)_2$, $CMe_2(CF_3)$ or $CMe(CF_3)_2$]. The compounds can be distilled *in vacuo* as colorless liquids. More easily handled solid derivatives, which can be isolated as colorless crystals, were prepared by reacting the dimethylamine adducts with 4-dimethylaminopyridine to give $M(OR_f)_3(4\text{-}Me_2Npy)$ [M = Al or Ga; $R_f = CH(CF_3)_2$, $CMe_2(CF_3)$ or $CMe(CF_3)_2$]. X-Ray crystallographic studies of $Ga[OCH(CF_3)_2]_3(4\text{-}Me_2Npy)$, $Ga[OCMe_2(CF_3)]_3(4\text{-}Me_2Npy)$ and $Al[OCMe(CF_3)_2]_3(4\text{-}Me_2Npy)$ showed they have distorted tetrahedral geometries. Gallium oxide films were prepared from $Ga[OCH(CF_3)_2]_3(HNMe_2)$ and air by low pressure chemical vapor deposition at substrate temperatures of 250–450 °C. The highest quality film was deposited at 450 °C. Its composition was $Ga_2O_{3.1}$ by backscattering analyses and the growth rate was ≈3800 Å min^{-1}. The film had an optical band gap of 4.9 eV, which is close to the value reported for bulk material (4.8 eV), and it was >90% transmittant in the 300–820 nm region.

This and our recent studies[21] involving depositions using $Sn[OCH(CF_3)_2]_4(HNMe_2)_2$ and $Sn[OCH(CF_3)_2]_2(HNMe_2)$ precursors suggest that fluorinated alkoxide complexes are promising precursors to main group oxide thin films. In the present example, it remains to be determined whether $Ga[OCH(CF_3)_2]_3(HNMe_2)$ provides any significant advantage over non-fluorinated alkoxide derivatives, such as $[Ga(\mu\text{-}OR)(OR)_2]_2$ [R = *i*-Pr (bp 120 °C/1.0 mm Hg) or *t*-Bu (subl. 140–150 °C/0.5 mm Hg),[23–27] or their ligand adducts. The volatile trialkyl gallium complexes $GaMe_3$ and $GaEt_3$ are also potential precursors to gallium oxide films but they are pyrophoric, and it should be noted that the indium congener $InMe_3$ did not produce films when combined with oxygen in a thermal low pressure CVD process.[28]

Acknowledgements

This work was supported in part by the Robert A. Welch Foundation, Environmental Institute of Houston, MRSEC Program of the National Science Foundation under Award Number DMR-9632667 and by the State of Texas through the Texas Center for Superconductivity at the University of Houston and the Advanced Research Program. We thank Dr. James Korp for his technical assistance with the crystal structure determination of **11** and his helpful discussions.

References

1 M. Fleischer and H. Meixner, *Sens. Actuators B*, 1992, **6**, 257.
2 M. Fleischer and H. Meixner, *Sens. Actuators B*, 1991, **4**, 437.
3 G. A. Battiston, R. Gerbasi, M. Porchia, R. Bertoncello and F. Caccavale, *Thin Solid Films*, 1996, **279**, 115.
4 K. M. Waggoner, M. M. Olmstead and P. P. Power, *Polyhedron*, 1990, **9**, 257.

5 H. Nöth and P. Konrad, *Z. Naturforsch.*, *B: Chem. Sci.*, 1975, **30**, 681.
6 MolEN, An Interactive Structure Solution Program, Enraf-Nonius, Delft, 1990.
7 RUMP: based on L. R. Doolittle, *Nucl. Instrum. Methods Phys. Res.*, *Sect. B*, 1985, **9**, 344.
8 M. B. Power, J. W. Ziller and A. R. Barron, *Organometallics*, 1993, **12**, 4908.
9 E. C. Onyiriuka, S. J. Rettig, A. Storr and J. Trotter, *Can. J. Chem.*, 1987, **65**, 782.
10 M. A. Petrie, M. M. Olmstead and P. P. Power, *J. Am. Chem. Soc.*, 1991, **113**, 8704.
11 W. M. Cleaver and A. R. Barron, *Organometallics*, 1993, **12**, 1001.
12 M. D. Healy, J. W. Ziller and A. R. Barron, *J. Am. Chem. Soc.*, 1990, **112**, 2949.
13 M. H. Chisholm, V. F. DiStasi and W. E. Streib, *Polyhedron*, 1990, **9**, 253.
14 M. D. Healy, M. R. Mason, P. W. Gravelle, S. G. Bott and A. R. Barron, *J. Chem. Soc.*, *Dalton Trans.*, 1993, 441.
15 M. D. Healy, D. A. Wierda and A. R. Barron, *Organometallics*, 1988, **7**, 2543.
16 M. D. Healy, J. W. Ziller and A. R. Barron, *Organometallics*, 1991, **10**, 597.
17 M. B. Power, S. G. Bott, D. L. Clark, J. L. Atwood and A. R. Barron, *Organometallics*, 1990, **9**, 3086.
18 A. P. Shreve, R. Mulhaupt, W. Fultz, J. Calabrese, W. Robbins and S. D. Ittel, *Organometallics*, 1988, **7**, 409.
19 S. A. Sangokoya, W. T. Pennington, J. Byers-Hill, G. H. Robinson and R. D. Rogers, *Organometallics*, 1993, **12**, 2429.
20 R. H. Cayton, M. H. Chisholm, E. R. Davidson, V. F. DiStasi, P. Du and J. C. Huffman, *Inorg. Chem.*, 1991, **30**, 1020.
21 S. Suh, D. M. Hoffman, L. Atagi, D. C. Smith, J.-R. Liu and W.-K. Chu, *Chem. Mater.*, 1997, **9**, 730.
22 M. R. Lorenz, J. F. Woods and R. J. Gambio, *J. Phys. Chem. Solids*, 1967, **28**, 403.
23 R. Reinmann and A. Tanner, *Z. Naturforsch.*, *B: Chem. Sci.*, 1965, **20**, 524.
24 S. R. Bindal, P. N. Kapoor and R. C. Mehrotra, *Inorg. Chem.*, 1968, **7**, 384.
25 S. R. Bindal, P. N. Kapoor and R. C. Mehrotra, *J. Chem. Soc. A*, 1969, 863.
26 J. G. Oliver and I. J. Worrall, *J. Chem. Soc. A*, 1970, 845.
27 J. G. Oliver and I. J. Worrall, *J. Chem. Soc. A*, 1970, 2347.
28 T. Maruyama and T. Kitamura, *Jpn. J. Appl. Phys.*, 1989, **28**, L1096.

Paper 8/08460B